Determination of detonation front curvature radius of ANFO explosives and its importance in numerical modelling of detonation with the Wood-Kirkwood model

Štimac Tumara, Barbara; Dobrilović, Mario; Škrlec, Vinko; Sućeska, Muhamed

Source / Izvornik: **Rudarsko-geološko-naftni zbornik, 2022, 37, 97 - 107**

Journal article, Published version
Rad u časopisu, Objavljena verzija rada (izdavačev PDF)

https://doi.org/10.17794/rgn2022.2.9

Permanent link / Trajna poveznica: https://urn.nsk.hr/urn:nbn:hr:169:998562

MGPB

Determination of detonation front curvature radius of ANFO explosives and its importance in numerical modelling of detonation with the Wood-Kirkwood model

Rudarsko-geološko-naftni zbornik
(The Mining-Geology-Petroleum Engineering Bulletin)
UDC: 622.2
DOI: 10.17794/rgn2022.2.9

Original scientific paper

Barbara Štimac Tumara[1]; Mario Dobrilović[1]; Vinko Škrlec[1]; Muhamed Sućeska[1]
[1] *University of Zagreb, Faculty of Mining, Geology and Petroleum Engineering, Pierottijeva 6, 10 000 Zagreb, Croatia*

Abstract
Unlike most military high explosives, which are characterized by an almost plane detonation front, ammonium nitrate-based commercial explosives, such as ANFO (ammonium nitrate/fuel oil mixture) and emulsion explosives, are characterized by a curved detonation front. The curvature is directly related to the rate of radial expansion of detonation products in the detonation driving zone and the rate of chemical reactions, and it is one of the characteristics of nonideal explosives. The detonation theories used to model the nonideal behaviour of explosives require both reaction rate and rate of radial expansion to be known/specified as input data. Unfortunately, neither can be measured and what is mostly used is a link between these rates and parameters which can be more easily measured. In this paper, the Wood-Kirkwood approach of determination of radial expansion through the radius of detonation front curvature and the electro-optical technique for experimental determination of detonation front curvature of ANFO explosives is applied. It was shown that an experimentally determined radius of detonation front curvature *vs* charge diameter, incorporated in the Wood-Kirkwood detonation theory, can satisfactorily reproduce experimental detonation velocity-charge diameter data for ANFO explosives, especially when the pressure-based reaction rate law is also calibrated (D=1.3 and k=0.06 1/(μs/GPa^D)).

Keywords:
ANFO; nonideal detonation; detonation front curvature radius; detonation velocity; numerical modelling

1. Introduction

Based on conservation laws and hydrodynamic flow models, the Chapman-Jouguet (CJ) theory and the Zeldovich-von Neumann-Doering (ZND) theory are the two most used and generally accepted ideal detonation theories (**Fickett and Davis, 2000; Mader, 2007**). One of the main differences between them is that the CJ theory assumes instantaneous chemical reactions with no chemical reaction zone, while the ZND theory assumes the existence of a chemical reaction zone of definite length and duration (**Fickett and Davis, 2000**).

However, explosives whose behaviour cannot be accurately described by either of the two detonation theories are called nonideal explosives. Experimentally measured detonation velocities and pressures of those types of explosives are considerably lower than those obtained by calculations using ideal detonation. According to **Mader** (**2007**), nonideal explosives are those whose calculated detonation pressure differ from experimental pressure by more than 50 kbar and detonation velocity by more than 500 m/s. The main cause of the nonideal behaviour is a relatively long duration of chemical reactions in a chemical reaction zone (microseconds compared to nanosecond in case of ideal explosives), which directly results in a wide chemical reaction zone (tens of millimetres compared to micrometres in case of ideal explosives). This, in turn, results in radial energy loss in a detonation driving zone due to the divergent flow (see **Figure 1**). Radially lost energy results in a slower detonation propagation compared to those in an infinite charge diameter (**Esen, 2004; Mader, 2007**). Moreover, divergent flow directly impacts the detonation front shape. With a decrease of charge radius, the degree of front curvature increases up to a critical radius, where radial energy losses are too large so that steady-state propagation of detonation becomes impossible (**Higgins, 2012**). In addition to the divergent flow and curved detonation front, slow chemical reactions also result in other nonideal characteristics, such as nonlinear dependence of detonation velocity on charge radius, the existence of confinement and initial explosive density, the existence of a fraction of unreacted explosive at the end of the detonation driving zone, i.e. at the sonic line. On the other hand, with an infinitely large charge radius, radial energy losses are negligible, and the chemical reaction zone is narrow, there are no divergences from an axial flow, the detonation front is a plane, and the detonation approaches ideal behaviour. A typical example of nonideal explosives is ANFO, a mixture of ammonium nitrate (94-95 %) and fuel oil

Corresponding author: Barbara Štimac Tumara
e-mail address: barbara.stimac@rgn.hr

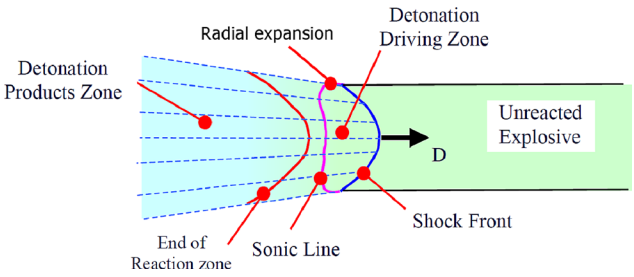

Figure 1. Graphical illustration of nonideal detonation **(modified from Peugeot and Sharp, 2002)**

(6-5 %), which is one of the most used commercial explosives.

1.1. Numerical modelling of nonideal detonation and the role of radial expansion model

To satisfactorily describe a nonideal detonation, a detonation model has to take into account the reaction rate and radial expansion rate of detonation products. In addition, it should be supplemented by equations of the state of unreacted explosive and detonation products. Several detonation theories are proposed so far. The most relevant are: Wood-Kirkwood (WK) slightly divergent flow steady-state kinetic detonation theory (**Wood and Kirkwood, 1954**), slightly divergent flow theory (**Kirby and Leiper, 1985**), detonation shock dynamics (DSD) (**Bdzil, 1981**) and straight streamline theory (**Sharpe and Braithwaite, 2005**). It should be noted that all detonation models developed based on these theories contain some degree of an engineering approach and empiricism.

One of the frequently used detonation theories is Wood-Kirkwood's slightly divergent steady-state kinetic detonation theory, which is based on Euler's hydrodynamic flow equations along the central streamline of a cylindrical charge of infinite length. One of the novelties, compared to the ZND detonation theory, introduced by Wood and Kirkwood is the radial expansion term (w) that describes the first-order perturbation from an ideal one-dimensional flow. However, direct experimental measurement of radial expansion is an impossible task. Radial expansion of the detonation products is most frequently regarded in relation to some other more easily measurable parameter. Wood and Kirkwood expressed a variation of radial expansion with flow velocity (*D-u*) by using the detonation front curvature radius (**Fried et al., 1998; Kirby and Chan, 2006**):

$$\omega = \frac{(D-u)}{R_c} \tag{1}$$

where:

ω – radial expansion term;
R_C – detonation front curvature radius (mm);
D – detonation velocity (km/s);
u – particle velocity in the moving frame (km/s).

The front curvature radius values tell us something about the nonideality of the detonation process: the smaller the value of curvature front radius, the larger the curvature and higher the degree of nonideality. On the other hand, a bigger curvature front radius means an approach to a flat front and ideal detonation.

The detonation front curvature radius can be either measured experimentally or estimated by some empirical equations. Various experimental setups for R_C measurements have been described in literature (**Catanach and Hill, 2002; Dorsett and Cliff, 2003; Kiyanda, 2010; Trzciński and Barcz, 2012; Pachman et al., 2016; Künzel et al., 2019**) but it sums down to registering the arrival of the detonation wave at the base of a cylindrical charge, with varying types of equipment used for measurement (high-speed camera, electronic counter, etc.). To calculate *Rc* from experimentally obtained detonation front lag *vs* charge radius data, several equations are proposed: circular equation (**Bogdanov et al.**, **2019**), quadratic equation (**Souers and Garza, 1998**), and the **Catanach and Hill** (**2002**) and **Jackson and Short** (**2015**) equations. The circular equation assumes the detonation front curvature is a regular circle, thus R_C remains the same along the charge radius. The derived radius is a direct input to the Wood-Kirkwood radial expansion model. However, other mentioned equations give a dependence of detonation front curvature along the radius of charge, meaning an additional equation is needed for the determination of the detonation front curvature radius at the central axis.

To incorporate the radial expansion model in nonideal detonation models, it is common to express the detonation front curvature radius as a function of charge radius. **Kennedy** (**1995**) proposed an equation that relates R_C with a charge diameter (d_0) and failure diameter (d_F). **Fried et al.** (**1998**) found that a slightly modified equation, which relates R_C with charge radius and failure radius (R_f), is adequate for various explosives:

$$\frac{R_o}{2R_c} = \alpha + \beta\frac{R_f}{R_o} \tag{2}$$

where:

R_0 – charge radius (mm);
R_C – detonation front curvature radius (mm);
R_f – failure radius (mm);
α and β – empirical constants.

Based on a large number of experimental data on R_C as a function of R_0 and R_f for various explosives, **Souers and Garza** (**1998**) found that α =0.0316 and β =0.178. Provided that R_f is known, **Equation 2** can be used for the estimation of R_C of any explosive.

Bdzil (**1981**) proposed an equation that relates R_C with charge diameter and chemical reaction zone width (x_{CJ}):

$$R_c = \frac{1}{\alpha}\left(d - \beta x_{CJ}\right) \tag{3}$$

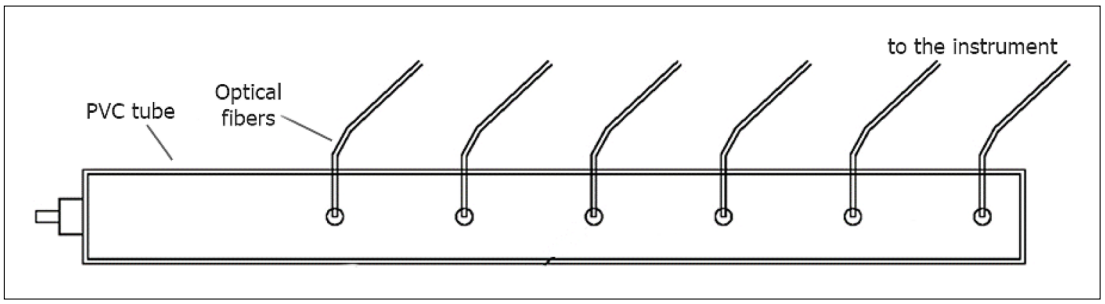

Figure 2. Experimental setup for detonation velocity measurements

where:

R_C – detonation front curvature radius (mm);
d – charge diameter (mm);
x_{CJ} – chemical reaction zone width (mm);
α and β – empirical constants.

Braithwaite et al. (1990) determined that for ANFO explosives constant α =0.5 and β =1.2. One of the disadvantages of this equation is the need for an experimentally measured chemical reaction zone width (x_{CJ}).

Detonation parameters of ANFO explosives depend on many factors: charge radius, the existence and characteristics of confinement, initial charge density and temperature, the size and porosity of ammonium nitrate prills, the initiation method, etc. In keeping all the factors unchanged and varying only the charge radius, it is possible to obtain the dependence of detonation velocity on charge radius. In this paper, the dependence of detonation velocity and detonation front curvature radius on unconfined ANFO charge radius is measured experimentally. So the obtained data are used for calibration of the radial expansion model and validation of the Wood-Kirkwood detonation model implemented in the EXPLO5 thermochemical code.

2. Experimental equipment and setup

Two separate experimental setups were used; one for the measurement of detonation velocity and another for the detonation front curvature of ANFO. The measurements are done on commercial ANFO explosives, consisting of 94.5% porous ammonium nitrate prills and 5.5% mineral oil. Typical bulk density varied from 0.80 to 0.88 g/cm^3. Four different rate sticks were fired in a thin wall (2.5 mm) PVC tubes having 71 mm, 105 mm, 120 mm, and 152 mm inner diameters for both experimental setups. The length of the charges was 100 cm, except for the 71 mm diameter where the length was 71 cm (ten times longer than the diameter). Three shots were fired for each charge diameter for the determination of detonation velocity and three shots for the determination of the detonation front curvature. ANFO charges were initiated by an electric detonator (720 mg of PETN) and a booster (APG20 with 20 g of PETN).

Both measurements of the detonation velocity and the front curvature were done by an electro-optical method

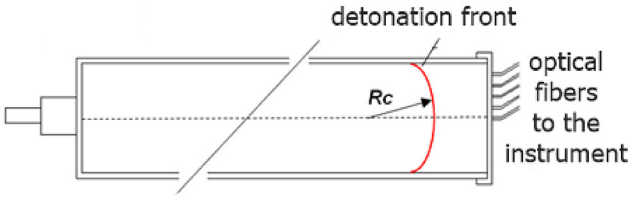

Figure 3. Experimental setup for detonation front curvature measurements

using detonation velocity meter "Explomet^2" (Kontinitro AS). Explomet^2 has 6 channels and a reading accuracy of ± 0.01 microseconds. The detonation velocity was measured by inserting optical fibres into holes drilled at equal intervals along the PVC tube. The detonation velocity at individual segments along the charge length is calculated from the known distance between neighbouring optical fibres (L) and measured time interval (Dt); D = L/Dt (see **Figure 2**).

To measure the detonation front curvature, the method described in **Pachman et al. (2016)**, **Bogdanov et al. (2019)**, **Künzel et al. (2019)** was used. According to the method, optical fibres are inserted in the fibre holder (custom 3D printed from PLA for each charge diameter) positioned at the charge base, opposite to the point of initiation (see **Figure 3**). The first optical fibre is located at the charge base central axis and others at equal distances along the charge radius. Given the curvature of the detonation front, the detonation wave arrives to the optical fibres, located at different radial distances, at different times. From the measured arrival time and previously measured detonation velocity for a given charge diameter, the data are transformed into detonation lag (in mm) *vs* radial distance.

2.1. Detonation velocity

The experiments have shown that detonation velocity (for 71-152 mm charge diameters) changes along its longitudinal axis, i.e. it decreases quickly and reaches a minimum value (at a distance of 200-300 mm from the point of initiation), after which it increases and reaches a constant value after approximately 5 charge diameters distance from the point of initiation. It should be noted, however, that the distance needed for the stabilization of detonation velocity, i.e. achieving steady-state detonation for a

given charge diameter, depends also on the type of booster (the higher the initial shock pressure, the faster the stabilization (**Cudzilo et al., 1995**)), charge radius and type of confinement. For example, for a larger charge radius (and/or stronger confinement), the steady-state detonation is reached closer to the point of initiation than for a smaller radius (and/or lighter confinement).

Since this study deals with the steady-state detonation velocity for both validation of numerical modelling applying the Wood-Kirkwood model and calculation of detonation lag *vs* radial distance from the measured detonation front curvature data, the detonation velocities determined at distances larger than 5x the charge diameter were used in further analysis. The measured detonation velocities are given in **Table 1**.

Table 1: The measured steady-state detonation velocity of unconfined ANFO charge

Charge diameter *d* (mm)	**Measured steady-state detonation velocity *D* (km/s)**
71	1.23
105	2.95
120	3.13
152	3.67
5000 (a)	4.78
Note: the average density of unconfines ANFO explosive charges is 0.83 g/cm³ (a) calculated ideal detonation velocity at d→∞ using EXPLO5	

The measured detonation velocity of ANFO as a function of charge radius is shown in **Figure 4**, along with some literature-reported data (**Catanach and Hill, 2002; Souers and Vitello, 2004; Jackson and Short, 2015**). The shape of the *D vs* $1/R_0$ curve is characteristic of highly nonideal explosives. Generally, there is good agreement in detonation velocity-charge radius data from various authors, especially considering the initial densities of ANFO in the literature sources mentioned range from 0.8 g/cm³ to 0.93 g/cm³. Differences in densities, as well as possible differences in ammonium nitrate prills properties and measurement method uncertainties, are probably the main reasons why the experimental detonation velocity data shown in **Figure 4** slightly differ. For example, for the 50 mm charge radius, detonations velocities vary between 2.57 km/s and 2.97 km/s, i.e. about 14%. The difference decreases at larger charge radii and increases in the vicinity of the failure radius.

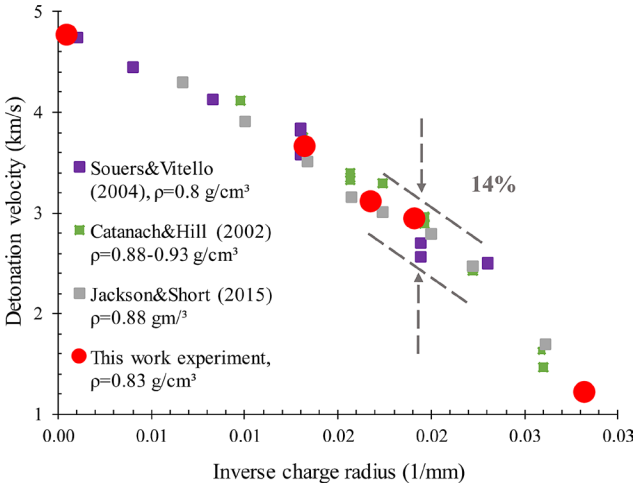

Figure 4. Measured and literature reported measured unconfined ANFO detonation velocity (*D*) data as a function of the inverse charge radius ($1/R_0$)

2.2. Detonation front curvature radius

Explomet[2] measures the time of arrival of the detonation wave to individual optical fibres located at different radial positions (see **Figure 3**). The detonation front lag *vs* radial position, $L_i(R)$ (see **Figure 5**), expressed in mm, is calculated from the measured arrival times and detonation velocity (**Bogdanov et al., 2019**):

$$L_i(R) = t_i(R) \cdot D \tag{4}$$

where:

$L_i(R)$ – detonation front lag dependent on radial position (mm);
$t_i(R)$ – measured arrival time (μs);
D – detonation velocity (km/s).

The detonation front lags *vs* radial position calculated from experimental data for all charge diameters are illustrated in **Figure 6**. It can be noticed that a significant scattering of the data points exists, especially at lower charge diameters. This can be related to various factors, such as the non-homogeneity of ANFO, the positioning of optical fibres, the effect of confinement for some charge diameters, etc. The charge diameter 71 mm shows a slight drop in curvature towards the edge. This can be linked to the fact that the speed of sound in the PVC tube (approx. 1.25 km/s) is close to the detonation velocity measured for that charge diameter. This in turn results in faster detonation propagation near the edge of the charge and flattening of the curvature. On top of that, the diameter of 71 mm (radius 35.5 mm) is close to the failure radius of the unconfined ANFO explosive, mean-

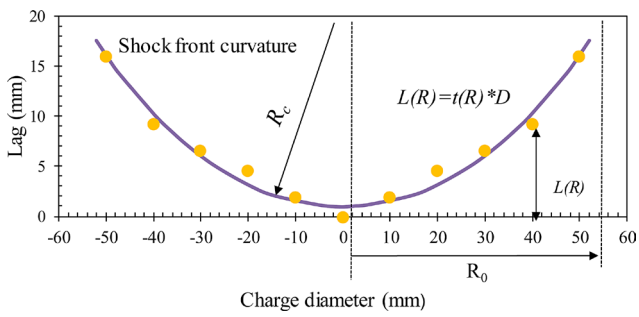

Figure 5. Detonation front lag *vs* radial position for 105 mm charge diameter

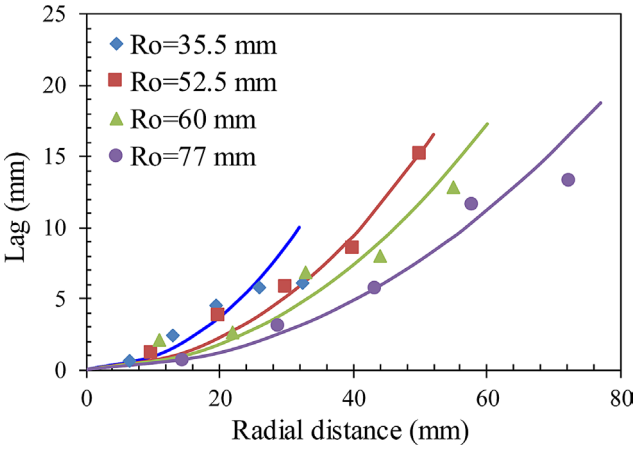

Figure 6. Detonation front lag *vs* radial distance for different charge radii

ing that the measured detonation velocity at that radius is close to unsteady propagation.

To derive the detonation front curvature radius from the measured lag *vs* radial distance data (see **Figure 6**), three different approaches are applied. Assuming the detonation wavefront has the shape of a regular circle, the radius of curvature can be derived using a circular equation (**Bogdanov et al., 2019**):

$$\sqrt{\left(X_P - X_C\right)^2 + \left(L_P - L_C\right)^2} = R_c \tag{5}$$

where:

X_P – x coordinate or radial distance R (mm);
X_C – x coordinate of the circle centre (on the axis X_C = 0) (mm);
L_P – y coordinate or lag (mm);
L_C – y coordinate of the circle centre on the axis (mm);
R_C – detonation front curvature radius (mm).

The second approach assumes the curvature can be described by a quadratic equation of the following form (**Souers and Garza, 1998**):

$$L_p(R) = AR^2 + BR^6 \tag{6}$$

where:

$L_p(R)$ – lag at radial distance R (mm);
R – radial distance from the central cylindrical axis (mm);
A and B are fitting constants.

The radius of curvature calculated from **Equation 6** varies with R according to the equation (**Souers and Garza, 1998**):

$$R_C = \frac{R}{2AR + 6BR^5} \tag{7}$$

and at the cylinder axis ($R \rightarrow 0$) equals:

$$R_C = \frac{1}{2A} \tag{8}$$

Lastly, the equation suggested by **Catanach and Hill (2002)**, which describes the detonation wave shape as a function of radius ($L_p(R)$), was also used:

$$L_p(R) = -\sum_{i=1}^{n} a_i \left(\ln\ln\left[\cos\cos\left[\eta \frac{\pi}{2} \frac{R}{R_0} \right] \right] \right)^i \tag{9}$$

where:

$L_p(R)$ – lag at radial distance R (mm);
R – radial distance from the central cylindrical axis (mm);
R_0 – charge radius (mm);
η and a_i – fitting parameters (with $0 \leq \eta \geq 1$ controlling the curvature near the edge of the charge), superscript i is taken to be 1 (no higher order fit is necessary).

The curvature can be calculated by equation (**Catanach and Hill, 2002**):

$$\kappa(R) = \frac{s'(R)}{\left(1 + s(R)^2\right)^{3/2}} + \frac{s(R)}{R\sqrt{1 + s(R)^2}} \tag{10}$$

$$s(R) = \frac{dL_P(R)}{dR} \tag{11}$$

where:

k(R) – curvature;
R – radial distance from the central cylindrical axis (mm);
$s(R)$ – the slope of the $L_p(R)$;
$L_p(R)$ – lag at radial distance R (mm).

The detonation front curvature radius at cylinder axis (R® 0) is calculated from the following relationship between the curvature and curvature radius for the axisymmetric cylinder geometry (**Higgins, 2012; Li et al., 2015**):

$$R_c = \frac{2}{\kappa(R \rightarrow 0)} \tag{12}$$

where:

R_C – detonation front curvature radius (mm);
k$(R \rightarrow 0)$ – curvature at cylinder axis.

The Wood-Kirkwood radial expansion model (**Equation 1**) considers the front curvature radius at the central axis, thus all three above-mentioned equations are applicable The difference between them is that the circular equation (**Equation 5**) gives the same front curvature radius at all radial positions, while both the quadratic equation (**Equation 7**) and the Catanach & Hill equation (**Equation 9**) give the curvature radius as a function of radial position R, and the front curvature radius at the central cylindrical axis (for R® 0) can be easily derived. The values of front curvature radii (R_C) at the central axis are obtained by fitting experimental lag *vs* radial position data (see **Figure 6**) to the above-described circular equation (**Equation 5**), the quadratic equation (**Equation 8**) and the Catanach & Hill equation (**Equation 12**). The results are given in given in **Table 2**.

Table 2: Calculated values of front curvature radii for different ANFO charge radii

Charge diameter d_0 (mm)	Charge radius R_0 (mm)	The radius of detonation front curvature R_C (mm) at $R \rightarrow 0$		
		Circular equation (5)	Quadratic equation (8)	Catanach & Hill equation (12)
71	35.5	56	35	52
105	52.5	91	91	89
120	60	115	98	120
154	77	167	119	178

The results given in **Table 2** show that the circular equation and the Catanach and Hill equation give very similar results, while the quadratic equation gives slightly different values for the 71 mm and 154 mm charges. In our opinion, this is because the quadratic equation is more sensitive to the significant scattering of $L_p - R$ data points. An additional reason is the small number of data points (six points) available for fitting $L_p - R$ dependence.

As mentioned before, it is common to express the detonation front curvature radius as a function of charge radius and failure radius (**Equation 2**). The equation proposed by **Fried et al. (1998)** (**Equation 2**) assumes a linear dependence of $(R_0/2R_C)$ on (R_f/R_0) (see **Figure 7**). It should be noted that the values of failure radius for unconfined ANFO reported in literature range from 31.5 mm (**Souers et al., 2004**) to 38.5 mm (**Jackson and Short, 2015**). Our experiments have shown that the steady-state detonation is possible at a 35.5 mm charge radius, thus in further analysis of $(R_0/2R_C)$ *vs* (R_f/R_0) dependence, a failure radius of 31.5 mm was taken. **Figure 7** illustrates $(R_0/2R_C)$ *vs* (R_f/R_0) dependence and gives

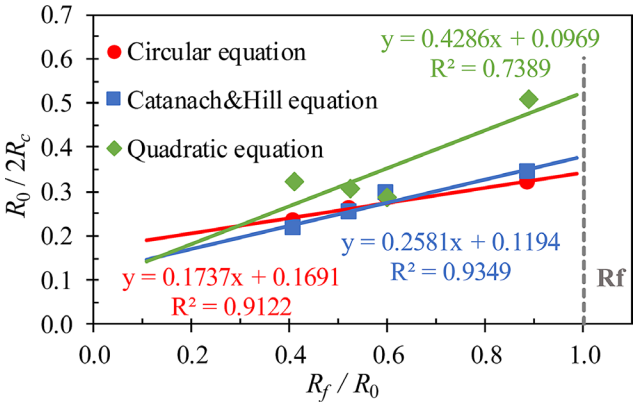

Figure 7. Linear dependence of $R_o / 2R_C$ on R_f / R_o for ANFO explosive

values of fitting constants *a* and b in **Equation 2**. The values of constant β for all three equations are reasonably close to those found by Souers (β=0.178), while values of constant α are much higher than Souers' value (α=0.0316). This means that, for the same charge radius, the curvature radii obtained in this work are significantly lower than those calculated by Souers' values of constants α and b.

A detailed analysis of R_C-R_0 experimental data reported by **Souers (1998)** has shown that a simple power-law equation describes R_C-R_0 data very well for many explosives:

$$R_C = \alpha \cdot R_0^{\beta} \tag{13}$$

where:

R_C – detonation front curvature radius (mm);
R_0 – charge radius (mm);
α and β – empirical constants.

The advantage of this dependence is that it does not require R_f to be known, but the disadvantage is that the constants α and b must be determined from R_C-R_0 experimental data for each explosive. The experimentally obtained R_C-R_0 data given in **Table 2** are fitted to **Equation 13** and so the obtained values of constants α and b for studied ANFO explosive are shown in **Figure 8** and summarized in **Table 3**.

The detonation front curvature radii of ANFO explosive *vs* charge radius determined in this work are compared with literature-reported data (**Bdzil et al., 2001; Catanach and Hill, 2002**) and with values calculated by Souers' empirical equation (**Souers, 1998**) in **Figure 9**. For this analysis, as well as for future calculations (in Section 3), the values obtained by the circular equation were used for two reasons. One is the fact that the circular and Catanach and Hill equations give almost the same values of the curvature radius and the second is the simplicity of the circular equation.

Table 3: Summary of empirical equations used to calculate R_C and values of fitting constants

	Equation	Fitting constants					
		Circular equation		Catanach&Hill equation		Quadratic equation	
		α	β	α	β	α	β
Souers' equation **(Eq.2)**	$\frac{R_o}{2R_c} = \alpha + \beta\frac{R_f}{R_o}$	0.1737	0.1691	0.2581	0.1194	0.4286	0.0969
Power law equation **(Eq.13)**	$R_c = \alpha * R_o^{\beta}$	0.3559	1.411	0.1688	1.5984	0.1252	1.6121

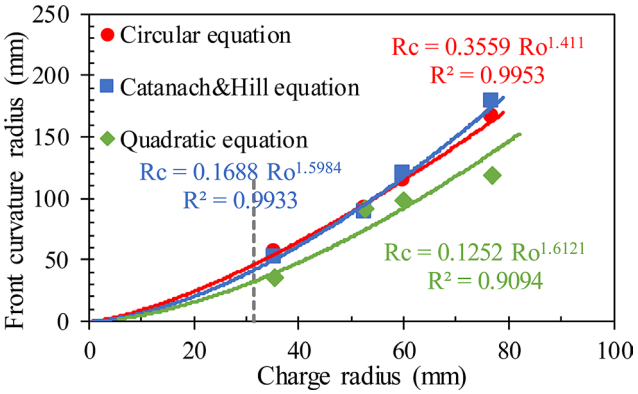

Figure 8. Power-law dependence of R_C on R_o for ANFO explosive

The quadratic equation proved to be more sensitive at a smaller number of points available for fitting, which, along with a significant scattering of L_p-R data point, resulted in a larger difference in R_C for some radii, compared to the other two equations. From **Figure 9**, it is visible that our values of R_C lie in between the literature experimental results of **Bdzil et al. (2001)** and **Catanach & Hill (2002)**, while Souers' empirical equation predicts significantly higher values of R_C at the same charge radius. Differences in curvature radius values from different authors can be attributed to differences in ANFO composition, properties of ANFO ingredients, differences in density, and the accuracy of the experimental method used.

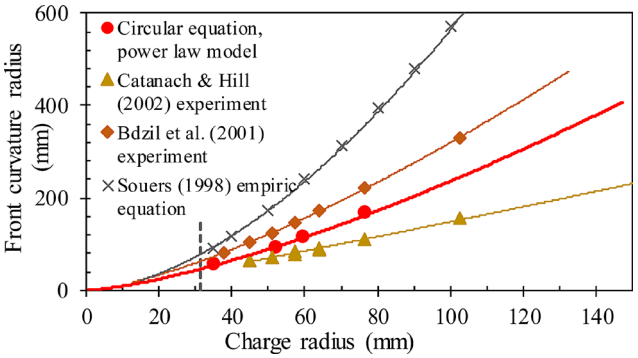

Figure 9. Calculated and literature R_C-R_o dependence data for unconfined ANFO explosive

3. Numerical modelling of ANFO charge diameter effect using the Wood-Kirkwood radial expansion model and power-law R_C-R_o dependence

The detonation front curvature data obtained in this work are used to model the nonideal behaviour of ANFO explosives and to predict the effect of charge diameter on detonation properties. Numerical modelling was performed using the EXPLO5 thermochemical code, coupled with Wood-Kirkwood's nonideal detonation theory, and supplemented with the reaction rate law, equations of state and the Wood-Kirkwood radial expansion model. The EXPLO5 code calculates the equilibrium composition of detonation products, parameters at the CJ state (i.e. sonic point), along the shock Hugoniot curve of detonation products and along the isentropic expansion of detonation products. The interaction between EXPLO5 and the Wood-Kirkwood model is described in detail in **Suceska (2018)** and **Stimac et al. (2020)**. Briefly, Wood-Kirkwood's differential flow equations are integrated for a specified detonation velocity, from the von Neumann spike down to the sonic point. For every integration step, i.e. volume and pressure state, the EXPLO5 code calculates the thermodynamical functions of products and unreacted explosives, product concentrations, energy derivations, total energy, etc. The detonation velocity is varied until the sonic condition is met and the pressure production parameter is close to zero (**Suceska, 2018**). The calculated detonation velocity (and other detonation parameters) is self-propagating steady-state detonation velocity for a specified charge diameter. It should be emphasized that this calculation only predicts the steady-state detonation velocity for an unconfined charge and does not describe initiation phenomena or the interaction of detonation products with the surroundings.

The EXPLO5 code uses Becker-Kistiakowsky-Wilson (BKW) equation of state of gaseous detonation products and the Murnaghan equation of state of condensed detonation products and unreacted ANFO (**Stimac et al., 2020**). The values of thermodynamical functions of ANFO explosives are derived from temperature-dependent enthalpy, which is used in EXPLO5 to calculate the internal energy and temperature of the compressed explosive (**Suceska, 2018**).

Along with the radial expansion rate, the rate of chemical reactions in the detonation driving zone is a key input parameter for the Wood-Kirkwood detonation model. Even though there are numerous reaction rate models proposed (**Peugeot and Sharp, 2002**), in this paper the calculations were done using a single-step pressure-based reaction rate law (**Sharpe and Braithwaite, 2005; Short et al., 2010**):

$$\frac{d\lambda}{dt} = k(1-\lambda)\left(\frac{p}{p_0}\right)^D \qquad (14)$$

where:

λ – mass fraction of reacted explosive (conversion);
t – time (μs);
k – reaction rate constant (μs/GPa^D);
p – pressure (GPa);
p_0 – initial reference pressure (1 GPa);
D – adjustable constant.

Using the power-law dependence of R_C on R_0 (see **Figure 8** and **Table 3**), obtained from the experimentally measured detonation front curvature and applying the circular equation to fit the obtained data, the rate constants k and D in **Equation 14** were adjusted to best re-

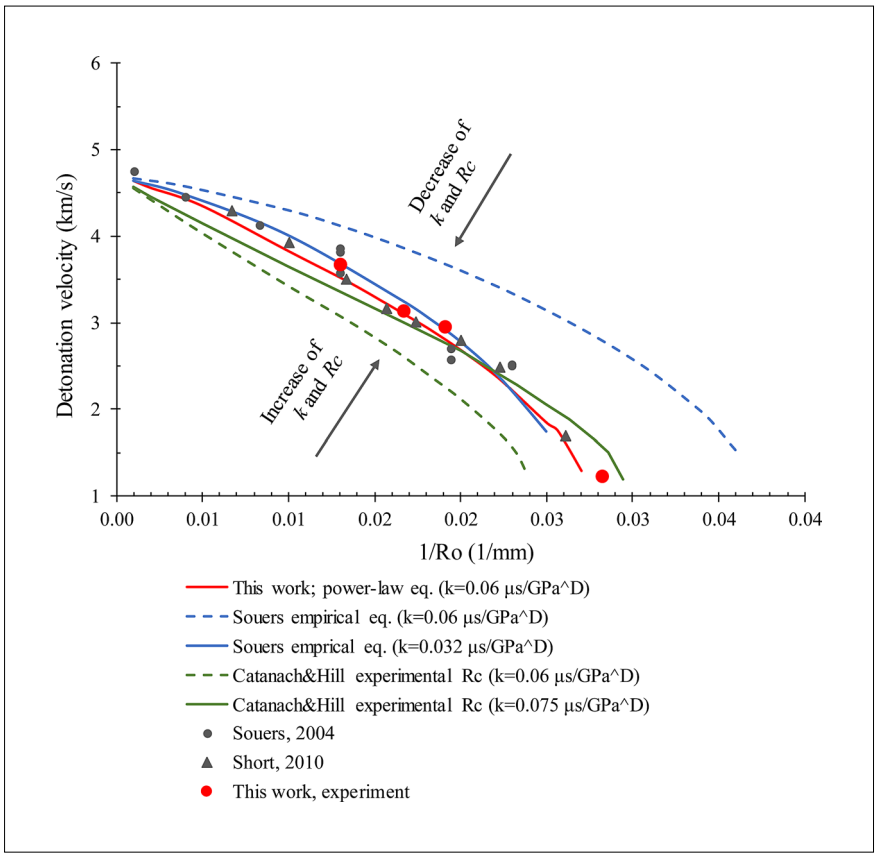

Figure 10. Effect of the detonation front curvature radius on predicted detonation velocity *vs* inverse charge radius (Note: rate constant *D* was equal to 1.3 in all calculations and experimental detonation velocities are taken from various sources)

produce the experimental detonation velocity *vs* the inverse charge radius curve. In this way, it was found that constants D=1.30 and k=0.06 1/(µs/GPa^D) result in the best agreement with the experimental detonation velocity – charge radius data (see **Figure 10**).

A continued decrease of detonation velocity from infinite radius towards failure radius is characteristic for highly nonideal explosives. Near the failure radius, the detonation velocity reaches only 40% of its value at an infinite charge radius (4.77 km/s). The detonation front curvature radius determined experimentally in this work, along with the rate constants calibrated in this work (k=0.06 µs/GPa^D, D=1.3) reproduces the experimental D-$1/R_0$ curve very well, even at the charge radii close to the failure radius where the Wood-Kirkwood theory is less valid (since it is based on a slightly divergent flow, while the flow is highly divergent close to the failure radius).

The detonation front curvature radii determined by **Catanach and Hill (2002)** (described for this study by the power-law equation R_C=0.98×$R_0^{1.09}$, with k=0.06 µs/GPa^D) underestimates detonation velocity for all charge radii. From Catanach and Hill's experimental data on the detonation front curvature, R_C=69.68 mm is determined for R_0=50 mm. This is 27% lower compared to our results. Such differences may be related to differences in ANFO compositions and properties of ANFO's ingredients. To a lesser extent, it may be related to the accuracy of the experimental setup and the data treatment procedure.

On the other hand, the detonation front curvature radii estimated by Souers' empirical equation (**Equation 2**)

Table 4: Effect of detonation front curvature radius and rate constant on calculation results (for R_o= 50 mm and ρ_o=0.8 g/cm^3)

Source of R_C data	R_C	k	**Calculated parameters**					
			D	p_{SP}	t_{SP}	x_{SP}	R_f	λ_{SP}
	(mm)	(µs/GPa$^{1.3}$)	(km/s)	(GPa)	(µs)	(mm)	(mm)	-
This work, experimental R_C	88.51	0.060	2.69	1.47	13.98	24.37	38	0.8869
Souers` empirical equation (**Equation 2**)	173.93	0.060	3.60	2.77	8.41	19.00	28	0.9548
	173.93	0.032	2.78	1.58	24.56	44.55	39	0.8953
Catanach&Hill (2002), experimental R_C	69.68	0.060	2.13	0.88	22.40	32.9	42	0.8151
	69.68	0.075	2.68	1.46	10.25	17.86	34	0.8582

Legend: p_{SP} is the detonation pressure at the sonic point, t_{SP} is the sonic time, x_{SP} is the width of the detonation driving zone and λSP is the conversion at the sonic point

overestimates the detonation velocity for all charge radii (see **Figure 10**). The constants in Souers' empirical equation (λ=0.0316, β=0.178) are derived from many experimental data for various explosives, most of them being ideal or less nonideal than ANFO. Given this, it is not surprising that Souers' values of constants cannot accurately predict R_C values for highly non-ideal ANFOs. **Table 4** shows that for R_0=50 mm, Souers' equation predicts R_C=173.93 mm, which is almost twice as much as we obtained (R_C=88.51 mm).

The differences in the properties of the ANFO ingredients can affect the rate of ANFO decomposition. It is found that an increase of rate constant from k=0.06 μs/GPa^D to k=0.075 μs/GPa^D will result in a much better agreement of the detonation velocity with the experimental results. Similarly, a decrease of the rate constant from k=0.06 μs/GPa^D to k=0.032 μs/GPa^D will result in a satisfactory agreement for Souers' empirical equation (see **Figure 10** and **Table 4**).

It is important to note from **Table 4** that even when the rate constant is adjusted to calculate the same or similar detonation velocity and pressure at the sonic point for R_0=50 mm, the width of the detonation driving zone and the sonic time remain quite different. In principle, the slower the reactions, the longer the reaction time and the wider the detonation driving zone. For illustration, for k=0.075 μs/GPa^D the width of the detonation driving zone is 17.86 mm, while for k=0.032 μs/GPa^D, the width of the detonation driving zone is 44.55 mm. This suggests that the validation of the nonideal detonation model cannot be done based on experimental D-$1/R_0$ data only, but must include an experimentally determined profile of the detonation driving zone, i.e. experimentally measured width of the detonation driving zone and sonic time.

4. Conclusions

This paper deals with the topic of improvement of nonideal detonation modelling to obtain more precise and reliable data to lessen the need for costly and time-consuming experimental research. Furthermore, the improvements in the numerical model give us a better understanding of the complex problem of explosive nonideality and the structure of the chemical reaction zone, which cannot be obtained by direct experimental measurements. In this paper, a cost-effective method of experimental determination of the detonation front curvature of ANFO explosives, and the procedure of evaluation of the radius of the curvature along the central axis are presented. The obtained radius of the curvature is used as input for the Wood-Kirkwood model of radial expansion, which is, in addition to the reaction rate law, crucial for the accurate modelling of a nonideal detonation.

It was demonstrated that the method based on the optical fibres-electronic counter technique can give the detonation front curvature of ANFO comparable with more sophisticated (and more expensive) methods that involve a high-speed camera. The methods of data processing to derive the detonation front curvature radius from the measurement can slightly affect the results. The description of the curvature by the circular equation seems to be the most adequate method to derive the curvature radius when small numbers of data points (in this case 6) are available for fitting experimental detonation lag *vs* radial distance data.

The curvature radii obtained in this work are comparable to literature-reported experimentally determined radii. For example, at R_0=50 mm, the difference goes up to 30%. In our opinion, several factors may affect such differences: variation in the properties of ANFO ingredients, variation in composition and density of the ANFO charges, accuracy of the experimental method used, and the data processing method. All these factors affect the reaction rates and consequently the detonation front curvature. The curvature radii estimated by Souers' empirical equation are significantly higher than the experimental, which means that the constants proposed by Souers cannot satisfactorily predict the curvature radii of ANFO explosives.

The dependence of the curvature radius on ANFO's charge radius can best be described by the power-law equation (R_C=0.356×$R_0^{1.411}$, with R^2=0.9953). The obtained R_C-R_0 dependence is incorporated in the Wood-Kirkwood nonideal detonation model coupled with the EXPLO5 thermochemical code and used to calibrate the rate constants. It was shown that the pressure-based reaction rate law, with D=1.3 and k=0.06 1/(ms/GPa^D) can reproduce experimental detonation velocity – inverse charge radius curve very well, even at the radii close to the failure radius.

It was demonstrated that reaction rate constants can be adjusted to reproduce the experimental detonation velocity-inverse charge radius curve for different detonation front curvature radii. This is logical given that the radial expansion of detonation products in the detonation driving zone is related to the rate of reactions. However, the results show that different rate constants predict different structures of the detonation driving zone (width and duration of the zone, reacted fraction of ANFO, etc.) although they predict the same values of detonation velocity and pressure for a given charge radius. This indicates that future research could focus on the proper calibration of the reaction rate constants and should include experimentally measured parameters in the detonation driving zone, mainly, pressure-time profile and duration and width of the zone.

Acknowledgement

This work has been supported by the Croatian Science Foundation (HRZZ) under the projects IP-2019-04-1618 "An improved nonideal detonation model of commercial explosives" (NEIDEMO).

5. References

Bdzil, J. B. (1981): Steady-state two-dimensional detonation. Journal of Fluid Mechanics, 108, 195–226.

Bdzil, J. B., Aslam, T. D., Catanach, R. A. and Hill, L. G. (2002): DSD front models: nonideal explosive detonation in ANFO. 12th International Detonation Symposium, San Diego, California, USA, 11th-16th April, 409-417.

Bogdanov, J., Andjelic, U., Bajic, Z., Brzic, S. and Nesic, J. (2019): Shape of detonation wave in different energetic materials based on nitrocellulose and nitroglycerine. Scientific Technical Review, 69, 2, 32–35. doi: 10.5937/str1902032b.

Braithwaite, M., Farran, T., Gladwell, I., Lynch, P. M., Minchinton, A., Parker, I. B. and Thomac, R. M. (1990): A detonation problem posed as a differential algebraic boundary value problem. Mathematical Engineering in Industry, 3, 1, 45–57.

Catanach, R. A. and Hill, L. G. (2002): Diameter Effect Curve and Detonation Front Curvature Measurements for ANFO. Mehlhorn, T.A., Sweeney, M.A. (eds.) AIP Conference Proceedings, 650, Albuquerque, New Mexico, USA, 23rd-28th June, 906–909. doi: 10.1063/1.1483684.

Cudzilo, S., Maranda, A., Nowaczewski, J. and Trzcinski, W. (1995): Shock initiation studies of ammonium nitrate explosives. Combustion and Flame, 102, 1–2, 64–72. doi: 10.1016/0010-2180(95)00011-T.

Dorsett, H. and Cliff, M. D. (2003): Detonation Front Curvature Measurements and Aquarium Tests of Tritonal Variants. Defence Science & Technology report DSTO-TR-1411, 45 p.

Esen, S. (2004): A non-ideal detonation model for commercial explosives. University of Queensland, 435 p.

Fickett, W. and Davis, W. C. (2000): Detonation Theory and Experiment. Dover Publications, INC., Mineola, New York, 386 p.

Fried, L. E., Howard, W. M. and Souers, P. C. (1998): Cheetah 2.0 User's Manual. Energetic Materials Center, Lawrence Livermore National Laboratory, 320 p.

Higgins, A. J. (2012): Steady one-dimensional detonations. in Zhang, F. (ed.) Shock Wave Science and Technology Reference Library. Springer-Verlag Berlin, 33–105. doi: 10.1007/978-3-642-22967-1.

Jackson, S. I. and Short, M. (2015): Scaling of detonation velocity in cylinder and slab geometries for ideal, insensitive and non-ideal explosives. Journal of Fluid Mechanics, 773, 224–266. doi: 10.1017/jfm.2015.240.

Kennedy, D. L. (1995): The Challenge of Non-Ideal Detonation. Journal de Physique IV Colloque, 05, C4, 191-207.

Kirby, I. J. and Chan, S. K. (2006): Analysis of VOD-diameter data using an analytical two-dimensional non-ideal detonation model. Furnish, M.D., Elert, M., Russell, T.P., White, C.T. AIP Conference Proceedings, 845, 1, Baltimore, Maryland, USA, 31st July- 5th August, 453–456. doi: 10.1063/1.2263358.

Kirby, I. J. and Leiper, G. A. (1985): A small divergent detonation theory for intermolecular explosives. 8th International Detonation Symposium, Albuquerque, New Mexico, USA, 15th-19th July, 176-186.

Kiyanda, C. B. (2010): Detonation modelling of non-ideal high explosives. University of Illinois, 247 p.

Künzel, M., Vodochodsky, O., Kucera, J. and Pachman, J. (2019): Simultaneous measurement of detonation velocity and detonation front curvature using fiber optic probe. Pachman, J., Selesovsky, R., Matyas, R. (eds.) 22nd Seminar of the New Trends in Research of Energetic Materials, Pardubice, Czech Republic, 10th-12th April, 503–508.

Li, J., Mi, X. and Higgins, A. J. (2015): Geometric scaling for a detonation wave governed by a pressure-dependent reaction rate and yielding confinement. Physics of Fluids, 27, 2, doi: 10.1063/1.4907267.

Mader, C. L. (2007): Numerical Modeling of Explosives and Propellants. 3rd edition. Boca Raton: CRC Press, 544 p.

Pachman, J., Kunzel, M., Kubat, K., Selesovsky, J., Marsalek, R., Pospisil, M., Kubicek, M. and Prokes, A. (2016): Optimex: Measurement of detonation front curvature with a passive fiber optical system. Central European Journal of Energetic Materials, 13, 4, 807–820. doi: 10.22211/cejem/62776.

Peugeot, F. and Sharp, M. (2002): NIMIC nations collaborative efforts in shock modelling - Reactive models for hydrocode: past, present and future. 5th International Symposium on High Dynamic Pressures, Saint Malo, France, 23rd-27th June, 127 p.

Sharpe, G. J. and Braithwaite, M. (2005): Steady non-ideal detonations in cylindrical sticks of explosives. Journal of Engineering Mathematics, 53, 1, 39–58. doi: 10.1007/s10665-005-5570-7.

Short, M., Quirk, J. J., Kiyanda, C. B, Jackson, S. I., Briggs, M. E. and Shinas, M. A. (2010): Simulation of detonation of ammonium nitrate fuel oil mixture confined by aluminum: Edge angles for DSD. 14th International Detonation Symposium, Idaho, USA, 11th-16th April, 769–778.

Souers, P. C. (1998): A Library of Prompt Detonation Reaction Zone Data. report UCRL-ID-130055 Rev 1, Lawrence Livermore National Laboratory, 35 p.

Souers, P. C., Vitello, P., Esen, S., Kruttschnitt, J. and Bilgin, H.A. (2004): The Effects of Containment on Detonation Velocity. Propellants, Explosives, Pyrotechnics, 29, 1, 19–26. doi: 10.1002/prep.200400028.

Souers, P. C. and Garza, R. (1998): Kinetic Information from Detonation Front Curvature. 11th International Detonation Symposium. Snowmass, Colorado, USA, 30th August-4th September, 459-465.

Souers, P. C. and Vitello, P. (2004): ANFO Calculations for Sedat Esen. report UCRL-TR-204259 Lawrence Livermore National Laboratory, 9 p.

Stimac, B., Skrlec, V., Dobrilovic, M. and Suceska, M. (2020): Numerical modelling of non-ideal detonation in ANFO explosives applying Wood-Kirkwood theory coupled with EXPLO5 thermochemical code. Defence Technology. doi: 10.1016/j.dt.2020.09.014.

Suceska, M. (2018): EXPLO5 Version V6.05 Users' Guide. Hrochuv Tynec, Czech Republic: OZM Research, 184 p.

Trzciński, W. A. and Barcz, K. (2012): Investigation of blast wave characteristics for layered thermobaric charges. Shock Waves, 22, 2, 119–127. doi: 10.1007/s00193-012-0357-z.

Wood, W. W. and Kirkwood, J. G. (1954): Diameter effect in condensed explosives. the relation between velocity and radius of curvature of the detonation wave. The Journal of Chemical Physics, 22, 11, 1920–1924. doi: 10.1063/1.1739940.

SAŽETAK

Određivanje polumjera zakrivljenosti fronte detonacijskoga vala ANFO eksploziva i njegova važnost u numeričkome modeliranju detonacije primjenom Wood-Kirkwoodova modela

Za razliku od većine vojnih visokih eksploziva, koje karakterizira gotovo ravna fronta detonacijskoga vala, komercijalne eksplozive na bazi amonijeva nitrata, kao što su ANFO i emulzijski eksplozivi, karakterizira zakrivljena fronta detonacijskoga vala. Zakrivljenost je izravno povezana s brzinom kemijskih reakcija i brzinom radijalnoga širenja produkata detonacije u zoni pokretanja detonacije i jedna je od karakteristika neidealnih eksploziva. Teorije detonacije, koje se koriste za modeliranje neidealnoga ponašanja eksploziva, zahtijevaju da se kao ulazni podatci znaju/specificiraju i brzina reakcije i brzina radijalnoga širenja. Nažalost, ni jedno ni drugo ne može se izmjeriti, pa se najčešće koristi veza između tih brzina i parametara koji se mogu lakše mjeriti. U radu smo primijenili Wood-Kirkwoodov pristup određivanja radijalnoga širenja preko polumjera zakrivljenosti fronte detonacijskoga vala te mogućnost eksperimentalnoga određivanja zakrivljenosti fronte detonacije ANFO eksploziva elektrooptičkom metodom. Pokazalo se da tako određen polumjer zakrivljenosti fronte detonacijskoga *vs* promjera naboja, ugrađen u Wood-Kirkwoodovu teoriju detonacije, može na zadovoljavajući način reproducirati eksperimentalne podatke o brzini detonacije i promjeru naboja ANFO eksploziva, pogotovo sa zadovoljavajućom kalibracijom modela brzine reakcija ovisne o tlaku (D = 1,3 i k = 0,06 1/(μs/GPa^D)).

Ključne riječi:
polumjer zakrivljenosti, brzina detonacije, ANFO, neidealna detonacija, numeričko modeliranje

Author's contribution

Barbara Štimac Tumara (PhD., Post-doctoral Researcher) performed EXPLO5 calculations, presentations and interpretation of the results. **Mario Dobrilović** (PhD., Professor) prepared and performed test samples and site testing. **Vinko Škrlec** (PhD., Associate Professor) prepared and performed test samples and site testing. **Muhamed Sućeska** (PhD., Professor) assisted in article conceptualization and data interpretation.